AUTOMATIC DOCKING MANOEUVRE AND ATTITUDE CONTROL SYSTEM

A Ercoli Finzi

Dip. Ingegneria Aerospaziale
Politecnico di Milano
Milan, Italy

F Venditti

Aeritalia, Gruppo Sistemi Spaziali
Torino, Italy

ABSTRACT

In this work the interaction between the automatic docking manoeuvre and the attitude dynamics of the involved spacecraft is analysed, as far as the docking manoeuvre behaviour is concerned. Three different docking concepts are investigated, by means of dedicated computer dynamics simulation programs. The simulations were run both considering rigid bodies and the presence of a flexible element between the docking port and the main body on one spacecraft; both with the docking port axis on each vehicle aligned with the center of mass and with large arms with respect to it. The need of proper attitude control systems has been established; the importance of energy dissipation sources has been evidentiated by the investigations.

Keywords: Automatic Docking, Attitude Control Law, Large Platforms, Energy Dissipation, Flexibility, Computer Simulations.

1. INTRODUCTION

The development of the most interesting future space activities in terms of scientific, technological and economic revenue, relies both on the on-orbit presence of large, multi-operative space stations and platforms and on the possibility to periodically maintain and supply them. The systematic and frequent performance of on-orbit construction/assembly and servicing may require the possibility to carry out simple and reliable/safe automatic docking manoeuvres (Ref. 1). This is indispensable for operations on geostationary orbit, but can be usefully considered for a wide range of low Earth orbit activities which do not necessarily involve the on-orbit man presence.
The docking manoeuvre performance involves a coupling in the dynamic behaviour of the two spacecraft due to the exchanged forces in the contact areas. This can have two consequences: on one side, the spacecraft could not be able to accept the new dynamics, due to attitude and accelerations conflicting with the operational requirements and strength characteristics; on the other side, the relative attitude and motion resulting from the coupled dynamics between the two spacecraft could lead to an abort of the docking manoeuvre itself. In this work, by means of computer dynamics simulations this last item has been investigated, i.e. the interaction between the docking manoeuvre and the attitude dynamics of the two bodies. This interaction depends heavily on the characteristics of the spacecraft (inertias, docking port positions) and on the chosen concept. Three different docking systems are analysed: a cone-cone one; a ring-conical truss one (these first two belonging to the soft docking class) and a non-impact deployable booms electromagnetic system. The latching mechanism, establishing the final structural connection is not considered, but the capability of the docking system to allow to reach very small distances (in the order of millimeters) while reducing initial relative errors is investigated. As far as the inertias and the configurations are concerned this work refers to a specific system, that is a large telecommunication platform studied in the previous years by ESA (Refs.2,3): it was conceived as a modular system composed by four elements connected by trusses, launched separately by Ariane and assembled in geostationary orbit by means of automatic rendez-vous and docking manoeuvres (Fig. 1). Particular emphasis has been placed in the study of the manoeuvre with a docking port on the target not aligned with the body center of mass and in considering the effect of flexible trusses on the target.

2. CONE-CONE CASE

The cone-cone system is analysed as an example of soft impact docking system. Two cone frustum elements, one as male, the other as female are placed on the vehicles (fig. 2): during the manoeuvre, the interactions between the surfaces are such that as the compenetration of the cones increases, linear and

Proceedings of the Second International Symposium on Spacecraft Flight Dynamics, Darmstadt, FR Germany, 20–23 October 1986 (ESA SP-255, Dec. 1986)

angular errors are reduced and pitch and yaw alignement is obtained. In this case a simplified approach resulting in a bidimensional treatment of the problem has been carried out, this representing a particular case of the docking of the central payload. A 2-D approach was considered sufficient for a first analysis of the system and the understanding of the main behaviours and problems. The spacecraft have been considered as rigid bodies and the impacts are treated according to the impulsive dynamics laws. With reference to the degrees of freedom described in fig.3 and assuming an inertial motion of the centers of mass (correct hypothesis if the manoeuvre time length is small with respect to the orbit duration)the assumed dynamics equations between two consecutive impacts are :

$$\begin{aligned} \ddot{x}_c &= 0 & \ddot{x}_t &= 0 \\ \ddot{y}_c &= 0 & \ddot{y}_t &= 0 \\ \ddot{\theta}_c &= 0 & \ddot{\theta}_t &= M/J_t \end{aligned} \qquad (1)$$

where M is the attitude control torque for the target, the first simulations showing the need for an attitude control system for the success of the manoeuvre, reducing the target rotations induced by the impacts. The chaser is not controlled in attitude. A simple linear-derivative control law has been chosen :

$$M = -[K(\theta_t - \bar{\theta}_t) + D\dot{\theta}_t] \qquad (2)$$

where $\bar{\theta}_t$ resents the nominal attitude. The control frequency ω and the damping time constant τ are related to the constants K and D by :

$$\omega = \sqrt{\frac{K}{J_t} - \frac{D^2}{4J_t^2}} \qquad \tau = \frac{2J_t}{D} = \frac{1}{\omega}\sqrt{\frac{1-\xi^2}{\xi^2}} \qquad (3)$$

Eq. 1 are integrated starting from the kinematic conditions resulting after each impact. Before the first impact, the conditions of the end of the rendez-vous phase are assumed: together with the approach relative velocity, V_a, the linear and angular misalignements ε and φ and their derivatives are considered. The maximum values of these errors are in agreement with the ones defines by ESA (Ref.4) In the impulsive hypothesis, the impact is instantaneous so that the configuration does not change; the values of the velocities of the two bodies after the impact (marked with the subscript +) are obtained from the ones before the impact (subscript -) from the equations of the impulsive mechanics, in the hypothesis of energy conservation :

$$\begin{aligned} m_t(\dot{x}_{t+} - \dot{x}_{t-}) &= I\gamma_x & m_c(\dot{x}_{c+} - \dot{x}_{c-}) &= -I\gamma_x \\ m_t(\dot{y}_{t+} - \dot{y}_{t-}) &= I\gamma_y & m_c(\dot{y}_{c+} - \dot{y}_{c-}) &= -I\gamma_y \\ J_t(\dot{\theta}_{t+} - \dot{\theta}_{t-}) &= I(P_{xt}\gamma_{yt} - P_{yt}\gamma_{xt}) & J_c(\dot{\theta}_{c+} - \dot{\theta}_{c-}) &= I(P_{xc}\gamma_{yc} - P_{yc}\gamma_{xc}) \end{aligned} \qquad (4)$$

$$\frac{1}{2}\left[m_t(\dot{x}_{t+}^2 + \dot{y}_{t+}^2) + J_t\dot{\theta}_{t+}^2 + m_c(\dot{x}_{c+}^2 + \dot{y}_{c+}^2) + J_c\dot{\theta}_{c+}^2\right] =$$
$$= \frac{1}{2}\left[m_t(\dot{x}_{t-}^2 + \dot{y}_{t-}^2) + J_t\dot{\theta}_{t-}^2 + m_c(\dot{x}_{c-}^2 + \dot{y}_{c-}^2) + J_c\dot{\theta}_{c-}^2\right]$$

where I is the impulse magnitude, $\bar{\gamma}$ its unit vector, $\bar{P}_t$ the vector from the target center of mass to the contact point and $\bar{P}_c$ the vector from the chaser center of mass to the contact point. To quantify the cones compenetration, a docking parameter has been introduced (fig. 4); as this parameter decreases the compenetration increases, and the alignement errors decrease; for the success of the manoeuvre the docking parameter must reach and maintain given minimum values, in such a way to allow the latching mechanism to operate. A first set of simulations showed the need for an attitude control system on the target: in fact without it, the minimum value of the docking parameter does not allow a successfull manoeuvre(fig. 5 where δ is the cone angle). Due to the large arms between the docking cone and the target center of mass, the impacts induce angular velocities such that the docking port is rapidly taken away from the one on the chaser.
After the introduction of the control system, an extended parametric analysis has been carried out to investigate the effects on the manoeuvre of several parameters: the cone aperture (δ =20° ÷ 140°), the approach velocity (V_a = 0.005 ÷ 0.03 m/s); the initial errors ($\varepsilon, \varphi, \dot{\varepsilon}, \dot{\varphi}$); the frequency ω of the control system (the damping ξ being always .7). The results have been statistically treated and they show an optimum cone angle of about 80°-90°; an optimum approach velocity as low as possible (0.005 m/s); a poor dependency of the final compenetration on the values of the initial misalignements and their derivatives ($\varepsilon, \varphi, \dot{\varepsilon}, \dot{\varphi}$). The main issue concerns the effect of the characteristics of the control system, exemplificated in fig. 6: the most the response of the control is quick, the most the manoeuvre is successfull. This can also be seen in fig. 7 where the distribution curves of the minimum docking parameter that can be reached, are plotted for two values of the frequency ω. It can be noted that an higher value of ω also means an higher energy dissipation rate.(Ref. 5).

3. RING-CONICAL TRUSS CASE

A different docking system has been considered to approach the three dimensional docking dynamics with an hertzian model for the computation of the contact forces. The system is represented by a proper description of finite cylinders and tori (fig. 8) which can model an actual system or represents a good discretization of the continuous elements (cone-cone) (but simplifying the 3-D impact detection algorithms). Cylinders and tori are described by their axes and director circumferences, surrounded by an interference envelope. The mathematical model can describe the dynamics of a generic system composed by n rigid bodies, connected by massless elements (rigid,flexible or exerting any user defined connection force) and subject to possible contact forces and control forces. The motion is described for each body by the evolution of the displacement vector $\{x_i\}$ of the center of mass with respect to the orbiting reference frame considered as inertial and of the director cosines $[A_i]$ of the local reference frame $O_i x_i y_i z_i$ coincident with the center of mass principal inertia axes, with respect to the orbiting frame. The motion equations take the form:

$$m_i \{\ddot{x}_i\} = \{F_i\}$$
$$[J_i]\{\dot{\omega}_i\} + \{\omega_i\} \wedge [J_i]\{\omega_i\} = \{M_i\} \quad (5)$$

where $\{\omega_i\}$ is the angular velocity vector, $\{F_i\}$ force vector, $\{M_i\}$ torque vector with respect to the center of mass and $[J_i]$ is the moment of inertia matrix. The action of control systems can be implemented and they produces torques $\{M\}$ in the form:

$$\{M\} = \{[K](\{\varphi\} - \{\varphi_0\}) + [D](\{\omega\} - \{\omega_0\})\} \quad (6)$$

where $\{\varphi_0\}$ and $\{\omega_0\}$ are nominal attitude and velocity values and $[K]$ and $[D]$ the control gains. The integration of eq. 5 is performed by means of a predictor-corrector method (Ref. 6), in which the predictor fixes a first tentative configuration, in order to compute the forces acting on each body. Both the predictor and the corrector use constant forces and torques during the integration step Δt, the former considering forces evaluated at the beginning of the step, the latter, their mean value inside the step. The exchanged forces between torus and cylinder have a component normal to the contact plane computed, according to the Hertz law, as a function of the radii, of the materials and of the compenetration of the two elements; a tangential friction component is also considered and its direction depends on the direction of the tangential component of the relative velocity in the contact area. In these assumptions, eq. 5 can be integrated as:

$$\{x_i\}_1 = \{x_i\}_0 + \{\dot{x}_i\}_0 \Delta t + \frac{1}{2}\{\ddot{x}_i\}\Delta t^2$$
$$[(1/\Delta t)[J_i] + [\{\omega_i\}_0 \wedge][J_i] - [J_i][\{\omega\}_0 \wedge]]$$
$$\{M_i\} - [\{\omega_i\}_0 \wedge][J_i]\{\omega_i\}_0 \quad (7)$$

where the indexes 0 and 1 refers to the beginning and to the end of the integration step. At the end of each step, the change in the attitude can be computed as:

$$\{\Delta\varphi_i\} = \{\omega_i\}\Delta t \quad (8)$$

and the unit vector of each axis $\{a_i\}$ (Ref.7) is computed as:

$$\{a_i\}_1 = [A_i]\{a_i\}_0 \quad (9)$$

where:

$$[A_i] = \{u_i\}\{u_i\}^T + \cos(\|\{\Delta\varphi_i\}\|)([I] - \{u_i\}\{u_i\}^T) + \sin(\|\{\Delta\varphi_i\}\|)[\{u_i\}\wedge] \quad (10)$$
$$\{u_i\} = \{\Delta\varphi_i\}/\|\{\Delta\varphi_i\}\|$$

The same reference configuration used for the cone-cone case has been adopted to perform the simulations (Ref. 8) in order to qualitatively compare the results (and to establish the validity of the 2-D approach). Fig. 9 shows the effect of different gain values on the docking parameter: the success of the manoeuvre requires an active control with an high damping, i.e. an high energy dissipation rate, as evidentiated in the 2-D case. Fig.10 shows that the material stiffness in the contact point has not a meaningful effect.

4. FLEXIBILITY EFFECTS

The introduction of flexible elements on the target, that is the truss connecting the main body to the docking port (fig. 11) has been implemented for the cone-cone case and the ring-conical truss case, in order to have a more realistic model of the system and to understand the effect of the flexibility. To reduce the computer time consumption, much greater for each run than for the rigid case, a small number of simulations has been carried out, corresponding to the best parameter values emerged from the rigid simulations. In the cone-cone case, three modes have been considered, with frequencies in the order of .1 ÷ 1 Hz. The motion equations have been written according to the Lagrangian approach, and have the form:

$$[m]\{\ddot{q}\} + [k]\{q\} = \{p\} \quad (11)$$

where $[m]$ and $[K]$ are the mass and stiffness matrices and $\{p\}$ the generalized force vector (Ref.12). The impulsive approach for describing the impact has been considered still applicable, as the estimated contact length is very small with respect to the periods of the target modes. In the ring-conical truss case, the presence of the flexible elements has been taken into account by means of connection forces whose values depend on the relative position/attitude between the two connected bodies. In both the two cases the structural damping has been also considered. The simulations show an improvement in the manoeuvre course with respect to the rigid case, due to the presence of the flexible truss. This can be seen in fig.s 12,13 for rigid and flexible simulations with the same attitude control system characteristics. It has to be pointed out that the improvement corresponds to the introduction of another source of energy dissipation, beyond the control system dissipation of the rigid case.

5. ELECTROMAGNETIC DEPLOYABLE BOOMS SYSTEM

An electromagnetic docking system was conceived as an example of a non-impact docking manoeuvre. The chaser is equipped with some flexible deployable booms, each with an electromagnet on the tip. A passive interface on the target is represented by permanent magnets properly placed (fig. 14). The booms length can be controlled independently for each boom. The manoeuvre involves the constant velocity booms deployment and the activation of the electromagnets and thus the rising of attractive forces which deforming the booms, bring near each electromagnet to the corresponding permanent magnet, till they join. At this point, the booms length control system allows the establishment of the nominal relative attitude recovering the linear and angular misalignements (in

the other presented cases, the target attitude was controlled with respect to an "inertial" frame, the relative alignements being obtained by means of the docking ports coupling). When the correct attitude is reached, the booms can be retrieved, allowing the final connection between the bodies. Three booms displaced at 120° each other represent the minimum number needed to allow to correct the misalignements in all the directions. The motion of the two bodies is described with respect to an orbiting reference frame always parallel to itself, so if $\bar{s}$ is the vector describing the position of the center of mass of one of the bodies of the system, the translational motion equations are (ref. 9):

$$\begin{aligned} m\,\ddot{s}_x &= F_x - m\,\omega_o^2\left\{s_x\left[1-3\cos^2(\omega_o t+\tau_o)\right]-\tfrac{3}{2}\,s_y\,\sin(2\omega_o t+2\tau)\right\} \\ m\,\ddot{s}_y &= F_y - m\,\omega_o^2\left\{-\tfrac{3}{2}\,s_x\,\sin(2\omega_o t+2\tau_o)+s_y\left[1-3\sin^2(\omega_o t+\tau_o)\right]\right\} \\ m\,\ddot{s}_z &= F_z - m\,\omega_o^2 s_z \end{aligned} \qquad (12)$$

(ω_o orbital angular velocity, constant as the orbit is considered circular, τ_o phase angle, $\bar{F}$ electromagnetic force). The angular velocity $\bar{\omega}$ for each body is obtained from the integration of the equation:

$$d\,/dt = \bar{M} \qquad (13)$$

($\bar{L}$ angular momentum, $\bar{M}$ external torque). The changes in the moments of inertia of the chaser, due to the booms motion, are also taken into account. The attitude is then computed by integration of (Ref.10):

$$\{\dot{\varphi}\} = \left[\phi\right]^{-1}\{\omega\} \qquad (14)$$

where $\{\varphi\}$ are the Euler angles and $[\phi]$ is the kinematic matrix:

$$[\phi] = \begin{bmatrix} -\sin\varphi_y & 0 & 1 \\ \cos\varphi_y \sin\varphi_x & \cos\varphi_x & 0 \\ -\cos\varphi_y \cos\varphi_x & \operatorname{sen}\varphi_x & 0 \end{bmatrix} \qquad (15)$$

The booms control system is an on-off one and works when all the booms are in contact with the target. A constant force is applied in the axial direction of the boom when:

$$\left|(\ell-\bar{\ell}) + \sigma\,\dot{\ell}\right| > K \qquad (16)$$

where $\bar{\ell}$ is a reference length (fig. 15).
The 3-D dynamic simulations refers to the configuration represented in fig. 14 (docking ports aligned with the bodies centers of mass). The results (Ref. 11) show that with a proper dimensioning of the control parameters the docking manoeuvre is feasable, and the target attitude is poorly perturbed and, anyway, quickly recoverable even starting from extreme initial errors (Ref. 4). In fig. 16 it can be seen that the corresponding Euler angles for the two spacecraft tend to the same value, i.e. the control system allows to reach the alignement of the vehicles. Two oscillating phases set up for short periods (about 10 s.): the first, between 25 and 40 s., corresponds to the establishment of the contacts between the three couples of magnetic poles; the second at 120 s. is due to the contemporaneous retrieval of the booms (fig. 17). The short duration of these oscillations, due to a proper dimensioning of the control system ($k=.01$, $\sigma=1$, $\bar{\ell}=1m$) does not jeopardize the dynamic stability of the system.

6. CONCLUSIONS

From the presented analysis, it emerges that the automatic docking manoeuvre involves perturbations in the attitude of the spacecraft, which could result in the abort of the manoeuvre. The presence of a control system with proper characteristics, can allow a sufficient reduction in the initial errors and the fulfillment of the geometric and kinematic conditions for the final latching. The importance of the presence of energy dissipation sources for the manoeuvre successfull course, has been also pointed out in this work.

7. REFERENCES

1. Vandenberg F.A. 1979, On Orbit Assembly of Large Space Structures (LSS) Using an Autonomous Rendez-Vous and Docking, AAS 79-100, Martin Marietta Aerospace, pp. 16

2. Aeritalia 1982, Ariane Dedicated Large Platforms for Telecommunication Payloads, LPA/RP/AI/004

3. Aeritalia 1982, Megalos: Mass Properties in Different Operational Configurations, LP-TN-AI-036

4. Briscol H.M. , Docking Mechanism Subsystem, Issue 2, ESA TPA/SPEC/44

5. Ercoli Finzi A.& Mantegazza P. 1984, Analisi preliminare della manovra di docking automatico con sistema a doppio cono, Rend. Istituto Lombardo, Accademia di Scienza e Lettere, vol.118

6. Giavotto V. et al 1983, Vehicle Dynamics and Crash Dynamics with Minicomputers, Computer and Structures, vol. 16

7. Faux I.D. & Pratt M.J. 1983, Computational Geometry for Design and Manufacture, Ellis Horwood, Chichester

8. Ercoli Finzi A. & Puccinelli L. 1985, Automatic Docking Feasability Analysis in Non-symmetric Conditions, VIII Congresso Nazionale A.I.D.A.A.

9. Wolverton R.W., Flight Performance Handbook for Orbital Operations, Wiley&sons

10. Hatkin B., Dynamics of flight (Stability and Control),Wiley & sons, Chap. 4

11. Ercoli Finzi A. & Albertini G., 1986, Dinamica della manovra di docking automatico con dispositivi elettromagnetici, A.I.D.A.A. 1° Convegno Italiano di Meccanica Computazionale, Milano

12. Giavotto V. , Strutture aeronautiche,CLUP-Milano

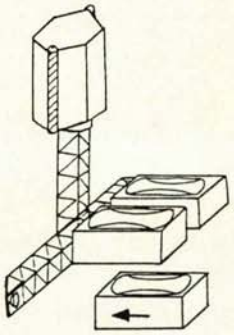

Figure 1. Reference Configuration

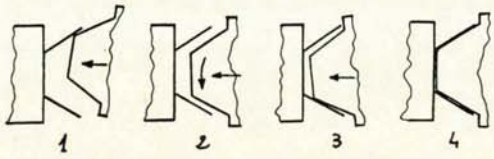

Figure 2. Cone-cone Case: Manoeuvre Sequence

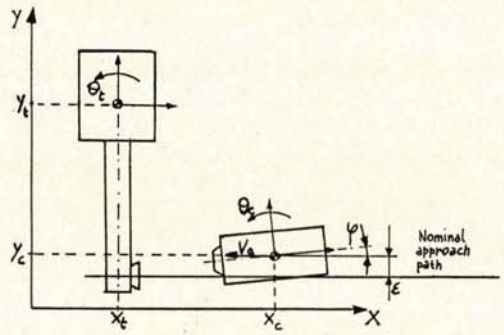

Figure 3. Cone-cone Rigid Case: Degrees of Freedom and Misalignements

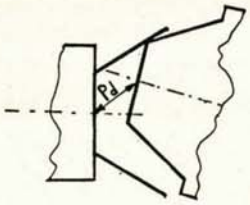

Figure 4. Docking Parameter

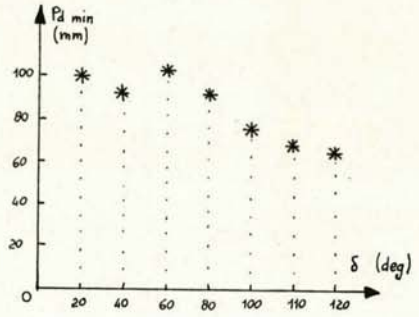

Figure 5. Cone-cone Rigid Case: Simulations without Control System

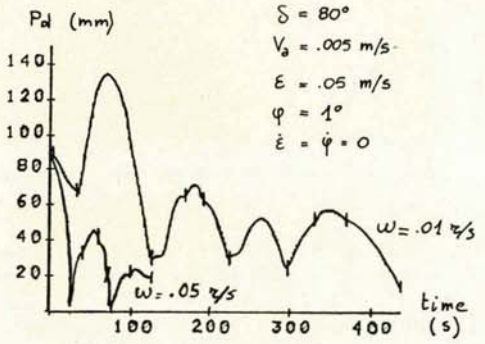

Figure 6. Cone-cone Rigid Case: Simulations with Different Control Characteristics

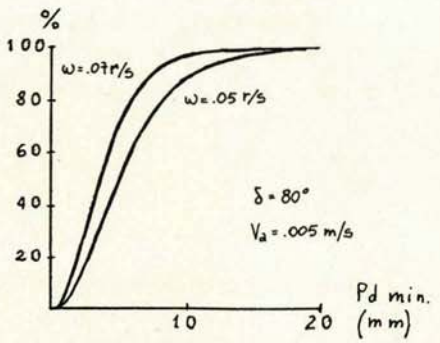

Figure 7. Cone-cone Rigid Case: Distribution Curves for Different Control Characteristics

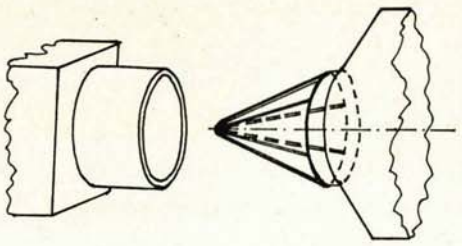

Figure 8. Ring-conical Truss Docking System

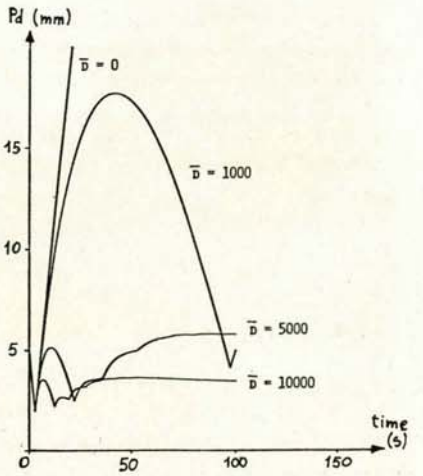

Figure 9. Ring-conical Truss Case: Simulations with Different Control Characteristics

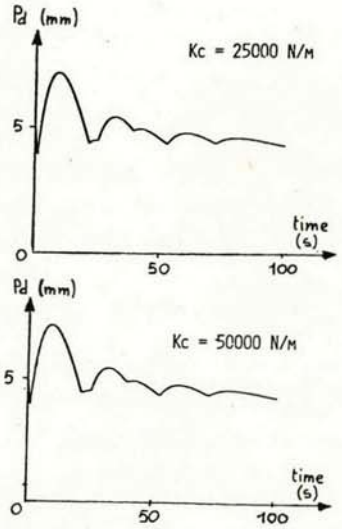

Figure 10. Ring-conical Truss Case: Simulations with Different Contact Stiffnesses

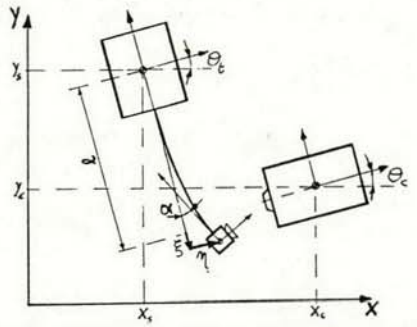

Figure 11. Introduction of the Flexibility of the Truss on the Target

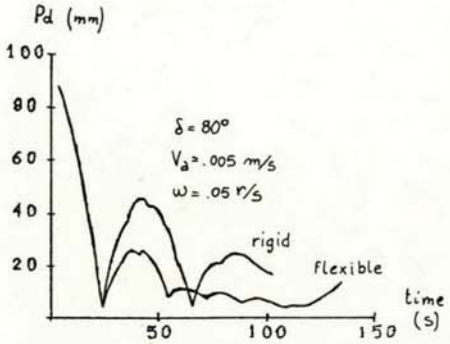

Figure 12. Cone-cone Elastic Case Compared with the Rigid Case

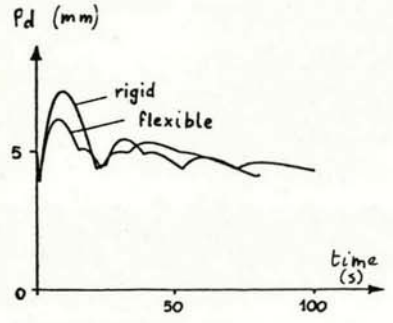

Figure 13. Ring-conical Truss Elastic Case Compared with the Rigid Case

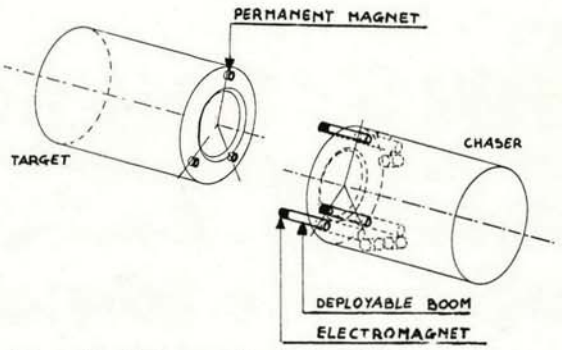

Figure 14. Electromagnetic Deploy able Booms Docking System

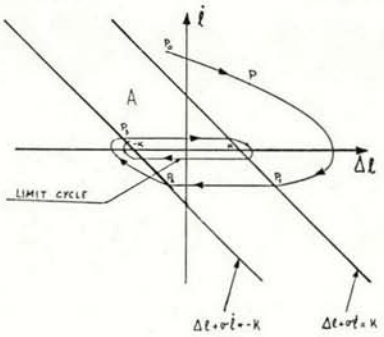

Figure 15. Electromagnetic System: Boom Length Control

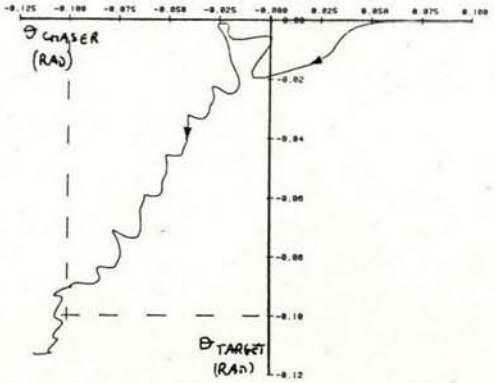

Figure 16. Electromagnetic System: Chaser ϑ Angle vs Target ϑ Angle

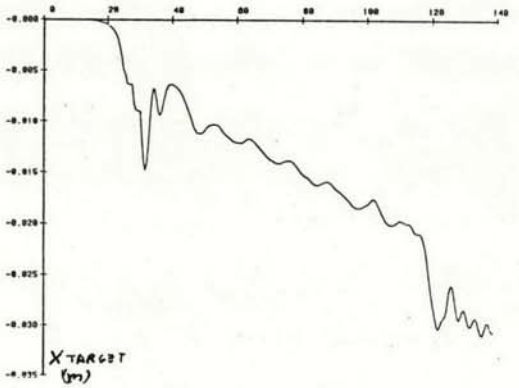

Figure 17. Electromagnetic System: Target Displacement